Aerosol and Air Quality Research, 13: 1313–1320, 2013

ISSN: 1680-8584 print / 2071-1409 online
doi: 10.4209/aaqr.2012.10.0269

Rapid Thermal Synthesis of Nano Titanium Dioxide Powders Using a Plasma Torch

Ya-Fen Wang[1], Hsing-Yuan Yen[2], Ying I. Tsai[3], Hong-Miao Chen[4], Cheng-Hsien Tsai[4*]

[1] *Department of Bioenvironmental Engineering, Chung Yuan Christian University, Chung-Li, Taiwan*
[2] *Department of Chemical and Biochemical Engineering, Kao Yuan University, Kaohsiung, Taiwan*
[3] *Department of Environmental Resources Management, Chia Nan University of Pharmacy and Science, Tainan, Taiwan*
[4] *Department of Chemical and Materials Engineering, National Kaohsiung University of Applied Sciences, 415 Chien-Kung Road, Kaohsiung 807, Taiwan*

ABSTRACT

Spherical TiO_2 nano- to microparticles are rapidly synthesized by spraying clear stock solution as a nano aerosol into an atmospheric-pressure microwave plasma torch at 550–600°C. The stock solution was prepared by an initial $H_2O/TiCl_4$ (titanium tetrachloride) volume ratio of 8. At about 0.15 s, anatase TiO_2 powders were produced and collected by 14-stage impactors. The size distribution shows that 98.47% of the particles in number were in the < 10-nm impactor, with the normalized particle number percentage ($dn'/d\log Dp$) of 327.1, although the mass distribution of the powders was mainly in the size range of 2.5–6.2 µm. Scanning electron microscopy and transmission electron microscopy images show that most of the spherical TiO_2 particles had a primary particle size of about 10 nm. Moreover, larger secondary particles (several µm), likely aggregated small particles were also presented. The chemical composition and elemental analyses show that the structure of the powders is mainly composed of TiO_2 with traces of TiO_2-xNx. Hence, the total reaction pathway is proposed as $Ti(OH)_xCl_{4-x} + H_2O + N_2 + O_2 \rightarrow TiO_2$ nuclei + HCl + other byproducts. Moreover, the ultraviolet-visible absorption spectrum and photocatalytic performance of the synthesized powders during exposure to ultraviolet or visible light are comparable to those of commercial TiO_2 powders.

Keywords: Synthesis; Photocatalyst; Nanoparticles; Size distribution; Discharge.

INTRODUCTION

Nanoparticles of TiO_2 photocatalyst for ultraviolet (UV) or visible light catalysis have great potential in the environmental and energy industries (Harizanov *et al*., 2001; Yu *et al*., 2002; Seery *et al*., 2007). TiO_2 is significant current interest for photocatalytic applications, such as the remediation of pollutants, water splitting, the destruction of highly toxic molecules, the selective and synthetically redox transformations, the production of hydrogen, and for the conversion of solar energy to electric power (Shie *et al*., 2009; Han *et al*., 2012; Chang *et al*., 2013).

Titania-based photocatalysts are usually prepared via liquid-phase or gas-phase synthesis. Commonly used liquid reaction approaches include the sol-gel method (Guan *et al*., 2001), the microemulsion method (Hsieh *et al*., 2008), the precipitation method (Parida *et al*., 2009), and the hydrothermal method (Cheng *et al*., 1995; Lu *et al*., 2008). In addition, by physical approach, larger TiO_2 stock powders carried by the high-speed airflow can be broken into nanoparticles under the action of crushing, friction and extrusion forces (Yang *et al*., 2012).

Titanium dioxide powders (5–400 nm) can be synthesized using a liquid-phase reaction. The advantage of liquid methods is easy control for producing nano-size particles and particle size uniformity. Drawbacks include long reaction time (1–24 h), complex processes or multiple stages, residual carbon matter, and high cost of precursors, such as TTIP ($C_{12}H_{28}O_4Ti$, C/Ti atom ratio = 12) and TEOT ($C_8H_{20}O_4Ti$, C/Ti atom ratio = 8) (Guan *et al*., 2001; Wang *et al*., 2006; Hsieh *et al*., 2008).

To reduce the reaction time (or residence time), gas-phase reactions can be conducted using a high-temperature flame aerosol method, such as premixed flame (Arabi-Katbi *et al*., 2001; Johannessen *et al*., 2001; Kammler *et al*., 2002; Tsantilis *et al*., 2002; Kammler *et al*., 2003), diffusion flame (Pratsinis *et al*., 1996; Akurati *et al*., 2007), and detonation processes (Ouyang *et al*., 2008a, b), by using TTIP or $TiCl_4$ as the feeds.

In addition, plasma approaches, such as radio-frequency

---

[*] Corresponding author. Tel.: +886-7-3814526 ext. 5110;
Fax: +886-7-3830674
E-mail address: chtsai@kuas.edu.tw

(RF) plasma (Nicholas *et al.*, 2009), microwave (MW) plasma (Hong *et al.*, 2005; Hong and Uhm, 2007), dielectric barrier discharge (DBD) (Chen *et al.*, 2007), and DC plasma (Li *et al.*, 2008; Vijay *et al.*, 2009), with gas-phase precursors have been proposed. Solid precursors (TiO_2 and Cu powders) for synthesizing Cu-doped TiO_2 also can be achieved by using a DC torch (Tsai *et al.*, 2013). The advantage of plasma methods is the fast plasma-chemical reaction with high electron or gas temperature, resulting in the reduction of activation energy and synthesis time. However, the operating conditions for the rapid gas-phase synthesis of titanium are not easy to control. In addition, the usage of precursors such as vaporized $TiCl_4$ or TTIP gas results in the emission of a large amount of Cl-containing compounds or the production of C-containing impurities in the particles (Chen *et al.*, 2007; Hong and Uhm, 2007; Li *et al.*, 2008). Moreover, the particle size distribution of TiO_2 powders, especially on the nano-to-micro scale, has not been studied extensively.

The present study uses an inexpensive reactant, $TiCl_4$, for the production of TiO_2 powders. Moreover, for reducing Cl atoms to remain or dope in the structure of as-prepared TiO_2 powders, the hydrolysis of $TiCl_4$ ($TiCl_4$ + H_2O) is utilized to remove the part of Cl atoms by producing HCl or Cl_2 and to form a clear, low-viscosity stock solution. The Cl atoms can be recovered and recycled for the production of $TiCl_4$. In addition, the stock solution, used as a source of precursors, was sprayed as a nano aerosol by an atomizer into a MW plasma reactor for rapidly (< 1 second) synthesizing mainly anatase-structure TiO_2 powders. Moreover, the mass and particle size distribution of the TiO_2 powders were determined to characterize the powders. Finally, the photocatalytic performance of as-synthesized powders was compared with that of commercial TiO_2 powders (Degussa, P25).

EXPERIMENT

A continuous MW plasma system (Fig. 1) was assembled with a commercially available magnetron (National Electronics YJ-1600, 2.45 GHz), whose maximum stationary power is 5 kW in continuous-wave mode. The microwaves passed through a circulator and a waveguide with a three-stub tuner, then reached a cavity with an arc to ignite the plasma. A quartz tube intersected the waveguide (ASTEX WR340) and a resonator was placed perpendicular to it. The gases in the axial gas were N_2 (1.5 standard liters per minute (slm)) and O_2 (1.5 slm). The flow rate of the swirl N_2 gas was 12 slm. The flow rate of the gas was regulated by a mass flow controller. Before the reaction, the chamber was flushed with mixing gases to remove residual impurities.

Titanium tetrachloride solution with an $H_2O/TiCl_4$ inlet volume ratio of 8 was sprayed as an aerosol into the reactor. A power of 900 W and temperatures of 550–600°C were used for producing TiO_2 powders. The powders were collected using a micro-orifice uniform deposit impactor (MOUDI, Model 110, MSP), with a working flow rate of 30.0 ± 0.2 L/min, combined with a downstream nano-micro orifice uniform deposit impactor (nanoMOUDI, Model 115, MSP), with a working flow rate of 10.0 L/min. The latter was used for collecting particles with sizes < 57 nm (Dp50% cutoff diameters of 32, 18, and 10 nm). Each sample set comprised 15 aerosol samples from micro to nano, with calibrated Dp50% cutoff diameters of 18 μm, 10 μm, 6.2 μm and 2.5 μm, 1.8 μm, 1.0 μm, 0.54 μm, 0.32 μm, 0.19 μm, 0.10 μm, 57 nm, 32 nm, 18 nm, 10 nm, and < 10 nm. Aluminum foils (47 mmφ, MSP) were used as the impact substrate and a quartz fiber filter (2500QAT-UP, 47 mmφ, pore size 0.8 μm, Pall) was placed at the base of the nanoMOUDI as an after-filter for collecting particles < 10 nm (Hsieh *et al.*, 2009). Although some powders in the nuclei mode may have diameters of around 3 nm, the smallest aerosol aerodynamic diameter is generally defined as 5 nm (McMurry and Woo, 2002). The particles collected on the quartz after-filter were thus designated as being in the 5–10 nm range.

The crystal structure of the as-prepared powders was determined using an X-ray diffraction (XRD) spectrometer (X'Pert PRO, MPD) with CuK_α radiation that scanned from 15° to 85° (2θ). The powders were also examined using a scanning electron microscope (SEM, Hitachi S3000N) and a high-resolution transmission electron microscope (TEM,

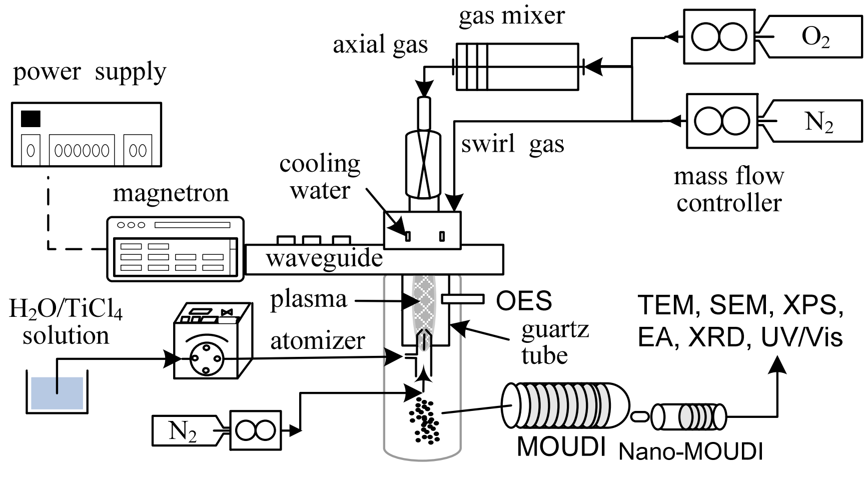

Fig. 1. Experimental apparatus.

Philips CM-200) to determine their size, morphology, and microstructure. The surface analyses and the determination of the chemical composition were performed using X-ray photoelectron spectroscopy (XPS, Fison ESCA210). An optical emission spectrometer (OES, Ocean Optics, HR 4000CG) was used to measure the active species involved in the formation of the powders in the discharge zone. The absorption spectrum and photocatalytic activity of the as-synthesized powders were measured using a UV-Visible spectrometer (PerkinElmer, V-670).

RESULTS AND DISCUSSION

Preparation of Clear Solution

In order to avoid blocking the atomizer, the precursors must be in the form of a clear and transparent liquid. Various $H_2O/TiCl_4$ volume ratios (4–26) were tested to prepare the clean solution and reduce the amount of Cl-containing compounds in the feedstock, Cl_2 and HCl in the gaseous effluents, and Cl atoms in the powders.

The results show that at an initial $H_2O/TiCl_4$ volume ratio of 8, the final stock solution with a $[Ti^{4+}]$ concentration of 1.14 M and a Ti/Cl atomic ratio of 0.9 is clear and transparent. Yellow and white precipitations were found for $H_2O/TiCl_4$ volume ratios of < 7 and > 10, respectively. Because $TiCl_4$ easily reacts with H_2O to form yellow $(Ti(OH)_xCl_{4-x})$ or white $(Ti(OH)_4)$ precipitation via the following reaction (Ritala *et al.*, 1993):

$$TiCl_4 + H_2O \rightarrow Ti(OH)_xCl_{4-x} + xHCl \qquad 0 \le x \le 4 \qquad (1)$$

The size distribution of aerosol particles fed into the plasma reactor was measured using a scanning mobility particle sizer (SMPS). The results show that the aerodynamic diameters were in the range of 20–300 nm, with a mean value of 46.1 nm. This clean solution can thus be sprayed as a nano aerosol by the atomizer into the glow discharge to react with O_2 in the plasma reactor.

Size Distributions of Mass and Particle Number of TiO_2 Powders

The size distribution of TiO_2 powders (in mass) was evaluated by calculating the mass sampled, the mass percentage, and the normalized mass percentage:

$$\text{Mass of } TiO_2 \text{ (M)} = \text{mass difference of filters before and after sampling} \qquad (2)$$

$$\text{Mass percentage of } TiO_2 \text{ (M')} = \text{M/total mass of powders} \times 100\% \qquad (3)$$

$$\text{Normalized mass percentage} = dM'/d\log Dp\ (\%) = dM'/d(\log Dp,u - \log Dp,l) \qquad (4)$$

M = mass (mg)
M’ = mass percentage (%)
$dM'/d\log Dp$ = normalized mass percentage (%)
Dp = midpoint particle diameter (μm) = (Dp,*u* + Dp,*l*)/2
Dp,*u* = upper channel diameter (μm)
Dp,*l* = lower channel diameter (μm)

The size distribution of particle number of TiO_2 powders was evaluated by calculating the mass distributions under the assumption that all powders have the same density.

$$\text{Particle number of } TiO_2\ (n) = M/(4/3\ \pi\ (Dp/2)^3) \times (1/\text{density of } TiO_2) \qquad (5)$$

$$\text{Particle number percentage of } TiO_2\ (n') = n/\text{total } TiO_2 \text{ particles} \qquad (6)$$

$$\text{Normalized particle number percentage} = dn'/d\log Dp\ (\%) = dn'/d(\log Dp,u - \log Dp,l) \qquad (7)$$

n = number of particles
n’ = particles number percentage (%)
Density of TiO_2 = 4.23 g/cm^3
$dn'/d\log Dp$ = normalized particle number percentage (%)

The mass-fractionated particle samples (0.005–50 μm) were collected by a 14-stage impactor (MOUDI + nanoMOUDI). The size distributions were then calculated.

Table 1 shows that the most of the mass was contributed by particles in the size of 2.5–6.2 μm, reaching 33.0% of the total mass with a normalized particle number percentage of 83.66. The second and third largest mass contributions were by particles in the size ranges of 6.2–10 μm and 1.8–2.5 μm, with total mass ratios of 27.63% and 14.59%, respectively. The total mass ratio of the former three samples reached 75.2%. Fig. 2(A) shows that the mass distribution has a single peak. The mass increases with increasing particle size until a peak at 2.5–6.2 μm, indicating an association with the growth of nuclei from the injected $Ti(OH)_xCl_{4-x}$ aerosol. Moreover, higher normalized mass percentages ($dM'/d\log Dp$) of 133.09 and 102.24 were also found at 6.2–10 μm and 1.8–2.5 μm, respectively, to be around of 2.5–6.2 μm.

Although the mass peak is in the micrometer range, Table 1 shows that 98.47% of the particles (in particles number) were collected in the 5–10 nm stage impactor, with a normalized particle number percentage ($dn'/d\log Dp$) of 327.1. This indicates that the plasma processing produces mainly nano powders via the nubulization, desolvation, volatilization, dissociation, reaction/recombination, and nuclei growth processes. Fig. 2(B) shows that the particles number percentage significantly decreases with increasing particle size. The second and third highest particle number peaks are at 10–18 nm and 18–32 nm, with normalized particle number percentages of only 4.4 and 1.0, respectively (Table 1 and Fig. 2(D)).

Morphology and Proposed Growth Process of Powders

The morphology and shape of the as-synthesized powders are nearly spherical with a primary particle size of 10 nm, as obtained from SEM (Fig. 3(A)) and TEM images (Fig. 3(B)). Agglomerated powders with a particle size of several μm (Fig. 3(C)) were produced when the nano aerosols were vaporized and reacted with O_2 to form nano TiO_2 particles in the discharge environment. The TiO_2 nuclei agglomerated and formed large clusters of thermal nanoparticles when the nanoparticles passed through the afterglow discharge zone and sampling line. The TEM image in Fig. 3(D) shows that the large particles are composed of many nano-size grains.

Table 1. Size distribution of mass and particle number of as-prepared TiO_2 powders.

Size distribution (μm)	Medium size, Dp (μm)	TiO_2 mass percentage, M' (%)	*dM'/d*log*Dp* (%)	TiO_2 particle number percentage, n' (%)	*dn'/d*log*Dp* (%)
0.005–0.01	0.008	0.56	1.85	**98.47**	**327.1**
0.01–0.018	0.014	0.04	0.16	**1.120**	**4.389**
0.018–0.032	0.025	0.05	0.22	**0.257**	**1.030**
0.032–0.056	0.044	0.11	0.45	0.096	0.395
0.056–0.1	0.078	0.29	1.16	0.046	0.182
0.1–0.19	0.145	0.04	0.14	0.0009	0.0033
0.19–0.32	0.255	0.81	3.57	0.0036	0.0160
0.32–0.54	0.430	1.45	6.37	0.0014	0.0060
0.54–1	0.770	2.42	9.05	0.0004	0.0015
1–1.8	1.400	6.33	24.79	0.00017	0.00067
1.8–2.5	2.150	**14.59**	**102.24**	0.00011	0.00077
2.5–6.2	4.350	**33.00**	**83.66**	0.00030	0.00008
6.2–10	8.100	**27.63**	**133.09**	0.000004	0.00002
10–18	14.00	10.41	40.79	0.0000003	0.0000009
18–50	34.00	2.27	5.12	0.0000000	0.0000001

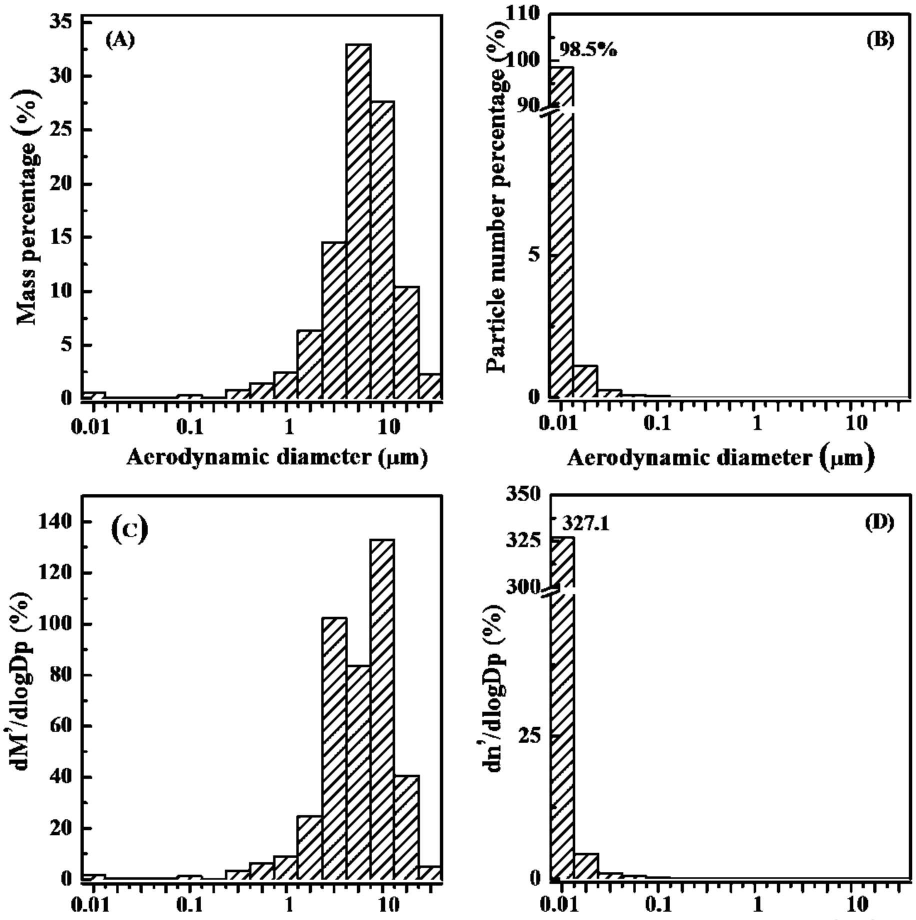

Fig. 2. Size distributions of (A) mass and (B) particle number with corresponding (C) normalized mass and (D) particle number percentages.

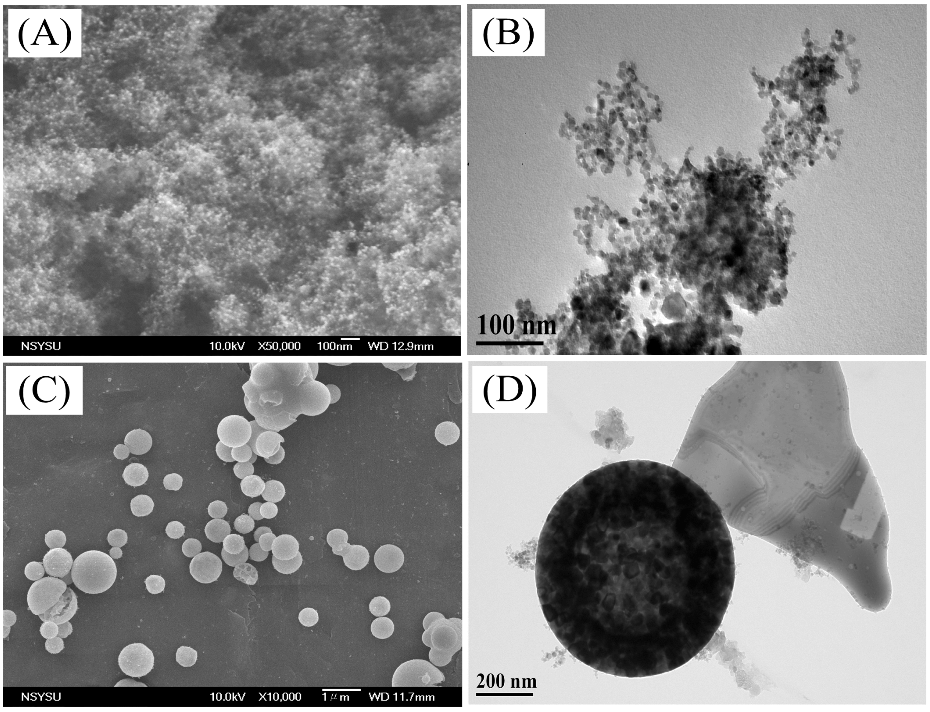

Fig. 3. Morphology of powders. (A) SEM and (B) TEM images of particles in 10–18 nm stage impactor; (C) SEM image of particles in 1–1.8 µm stage impactor; (D) TEM image of secondary particle as aggregation of primary particles.

XRD patterns (Fig. 4) show that the powders before and after sintering were mainly the anatase phase. Moreover, the average grain size calculated by XRD data is about 13–14 nm, to be consistent with the primary particle size, indicating that the larger secondary particles are aggregated mainly by the smaller primary particles. Ti atoms react with O to form crystalline TiO2 (anatase phase) at 550–600°C; however, amorphous TiO_2 existed in the as-prepared powders before calcination due to the short reaction time (about 0.15 s), resulting the weak peak was found in XRD patterns.

The proposed simplified reaction pathway is as follows:

$Ti(OH)_xCl_{4-x}$ aerosol in N_2/O_2 plasma at 550–600°C
→ $Ti(OH)_xCl_{4-x} + H_2O + N_2 + O_2$
→ TiO_2 nuclei + HCl + other gases (H_2O, N_2, O_2)
→ agglomerated TiO_2 powder

However, traces of TiO_xN_{2-x} powders were produced due to the active N-containing species possibly reacting with TiO_2 or doping TiO_2.

Surface Compositions and UV-Visible Spectrum of Powders

The surface compositions and functional groups of as-synthesized powders were measured by XPS. Elemental analysis shows that the N atom concentration was about 0.12 at.%, indicating N doping with a chemical bonding energy at 399.1 eV, corresponding to N_{1s}. This can be attributed to N-O bonds (Fig. 5(A)) (Guan *et al.*, 2001; Valentin *et al.*, 2005).

The O_{1S} peak region was deconvoluted into surface functional group contributions, as shown in Fig. 5(B). It was found that the O_{1S} peak can be fitted to two line shapes with binding energies at 529.2 and 531.2 eV, assigned to Ti-O and O-N bonds, respectively (Chen *et al.*, 2007). The total area of the O_{1S} peak was 91.75% Ti-O and 8.25% O-N. The peak regions of Ti at 463.7 eV and 458.0 eV correspond to $Ti_{2P1/2}$ and $Ti_{2P3/2}$, respectively, in the XPS spectrum (Fig. 5(C)), and can be attributed to the Ti-O functional group (Chen *et al.*, 2007). The total area of the Ti peak region was 27.36% $Ti_{2P1/2}$ (at 463.7 eV) and 72.64% $Ti_{2P3/2}$ (at 458.0 eV), respectively. These results

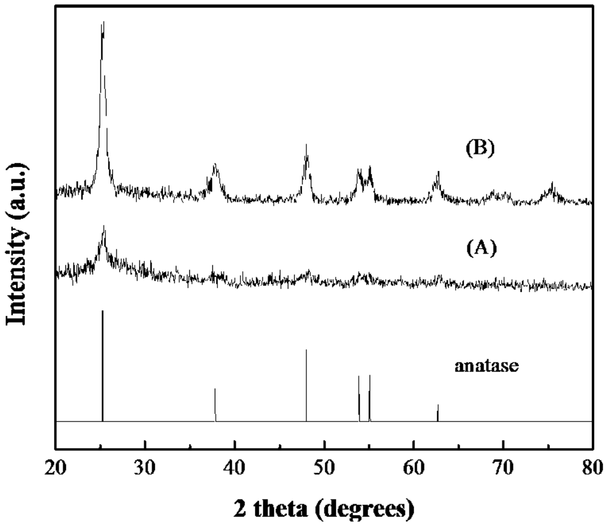

Fig. 4. XRD patterns of synthesized TiO_2 powders (A) before and (B) after calcination.

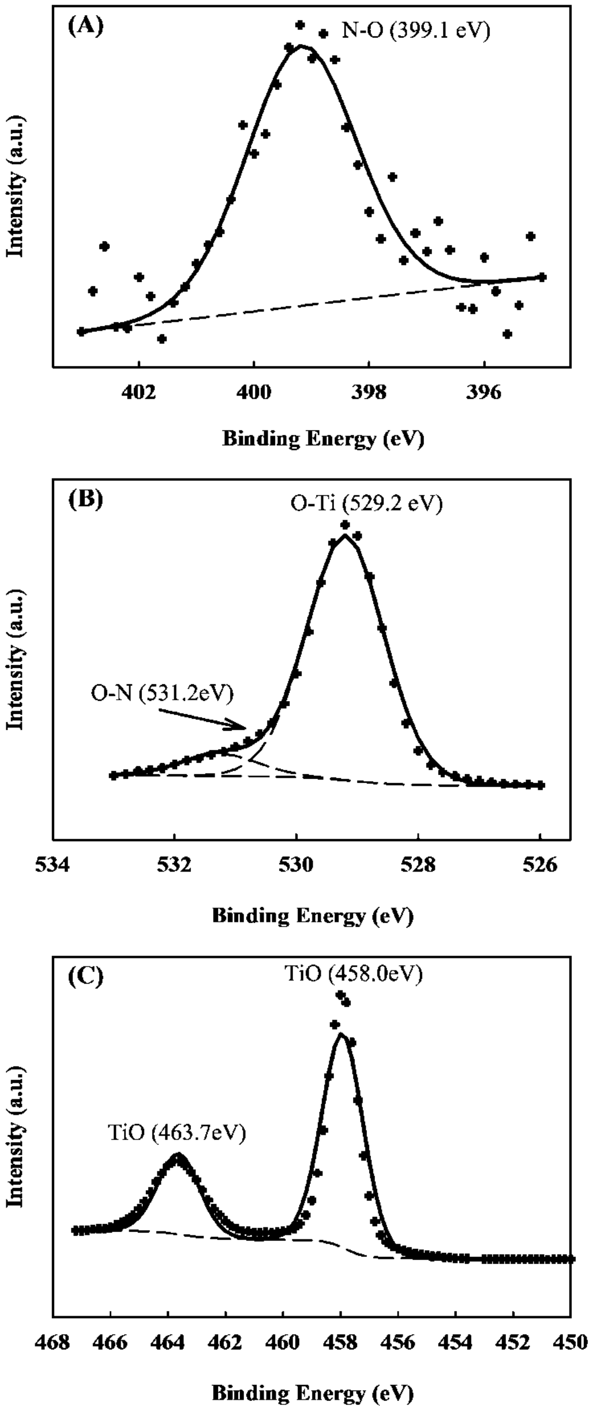

Fig. 5. XPS spectra of (A) N$_{1s}$, (B) O$_{1s}$, and (C) Ti$_{2p}$ for as-synthesized powders (dots: measured XPS data; dashed lines: fittings of binding energy spectra to XPS data; solid lines: sum of the fitted data).

suggest that the main functional groups for plasma-induced thermally synthesized titanium oxide powders are Ti-O bonds, with traces of O-N bonds. The powders are mostly composed of TiO$_2$ with some N-doped TiO$_2$-xNx.

The UV-Visible Kubelka-Munk absorption spectrum was measured to confirm the band gap and red shift of TiO$_2$ powders (Francisco *et al.*, 2000). Fig. 6 shows that

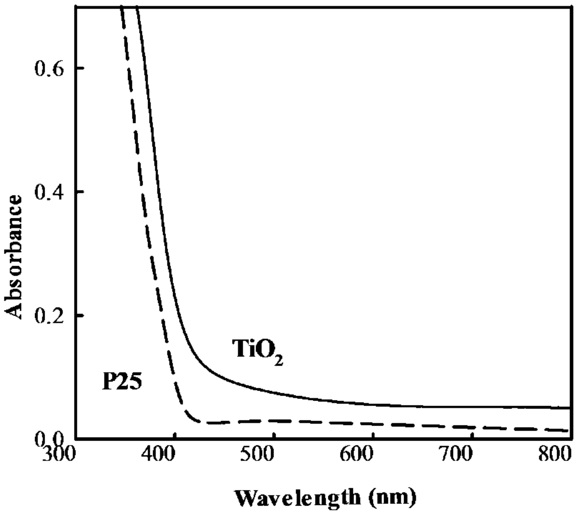

Fig. 6. UV-Visible Kubelka-Munk absorption spectrum of as-prepared TiO$_2$ powders and commercial P25 powders.

the band gap of the as-prepared powders was 410 nm, slightly higher than that (396 nm) of commercial P25 powders, and confirms that N-doped TiO$_2$ powders were produced by the rapid plasma thermal synthesis process.

The photocatalytic performance of the synthesized TiO$_2$ powders is comparable to that of commercial P25 powders for UV light degradation (Fig. 7(A)) and visible light degradation (Fig. 7(B)). This indicates that a MW plasma torch can be used for rapidly producing nano- and microparticle TiO$_2$ powders.

CONCLUSIONS

An atmospheric-pressure, high-temperature MW plasma torch was used to rapidly synthesize anatase TiO$_2$ particles with a size of about 10 nm by spraying a clear titanium chloride solution (Ti(OH)$_x$Cl$_{4-x}$) as a nano aerosol. This solution significantly reduced the emission of Cl-containing compounds, mainly HCl, during the synthesis process. Size-fractionated particle samples were collected and the results show that the percentage of particle number decreased with increasing particle size. Most particles were in size ranges of 5–10 nm, 10–18 nm, and 18–32 nm, with particle number percentages of 98.47%, 1.12%, and 0.257%, respectively. SEM and TEM analyses show that the powders had larger particles, which were agglomerated by primary particles when the TiO$_2$ nuclei passed through the afterglow discharge zone and sampling line. In addition, elemental analyses show that trace N atoms doped the structure of the powders, resulting in the production of TiO$_{2-x}$N$_x$ powders with a shift of the band gap from 396 nm to 410 nm.

ACKNOWLEDGMENTS

The financial support from the National Science Council of Taiwan under grants NSC 100-2221-E-151-004-MY2 and NSC 98-2221-E-151-009-MY2 is appreciated.

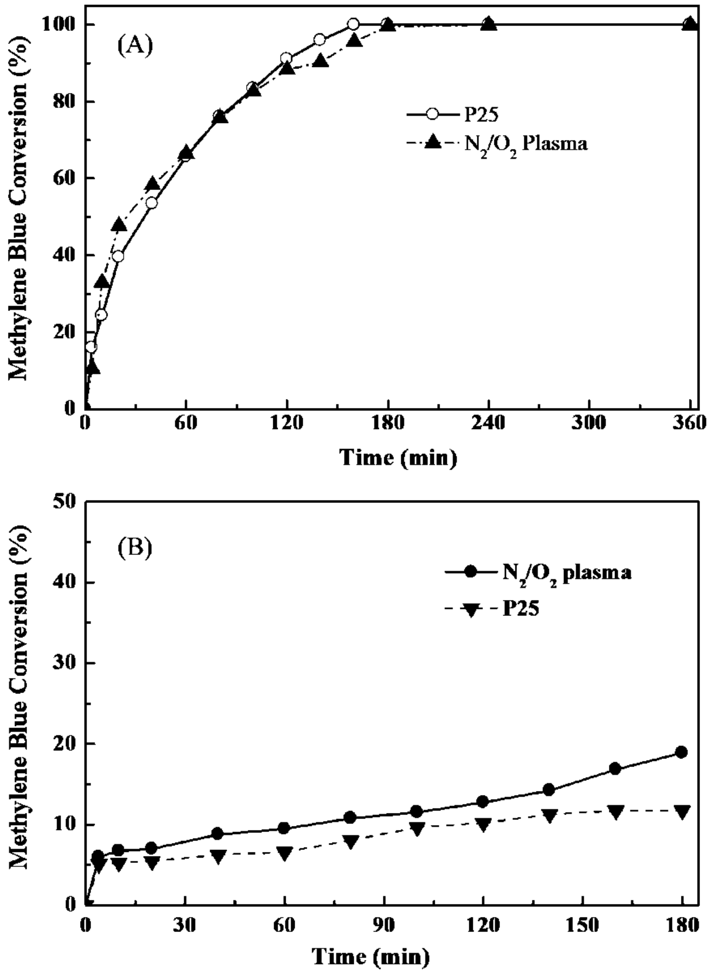

Fig. 7. Photocatalytic conversion of methylene blue for as-prepared (N_2/O_2 Plasma) and commercial TiO_2 powders (P25) under (A) UV light and (B) visible light irradiation ([MB] = 15 ppm, 10 mL).

REFERENCES

Akurati, K.K., Vital, A., Fortunato, G., Hany, R., Nueesch, F. and Graule, T. (2007). Flame Synthesis of TiO_2 Nanoparticles with High Photocatalytic Activity. *Solid State Sci.* 9: 247–257.

Arabi-Katbi, O.I., Pratsinis, S.E., Morrison, P.W. and Megaridis, C.M. (2001). Monitoring the Flame Synthesis of TiO_2 Particles by In-situ FTIR Spectroscopy and Thermophoretic Sampling. *Combust. Flame* 124: 560–572.

Chang, K.L., Sekiguchi, K., Wang, Q. and Zhao, F. (2013). Removal of Ethylene and Secondary Organic Aerosols Using UV-$C_{254\,+\,185\ \mathrm{nm}}$ with TiO_2 Catalyst. *Aerosol Air Qual. Res.* 13: 619–626.

Chen, C., Bai, H., Chang, S. and Chang, C. (2007a). Effect of Plasma Processing Gas Composition on the Nitrogen-Doping Status and Visible Light Photocatalysis of TiO_2. *J. Phys. Chem. C* 111: 15228–15235.

Guan, Z.S., Zhang, X.T., Ma, Y., Cao, Y.A. and Yao, J.N. (2001). Photocatalytic Activity of TiO_2 Prepared at Low Temperature by A Photo-Assisted Sol-Gel Method. *J. Mater. Res.* 16: 907–909.

Han, Z., Chnag, V.W.C., Zhang, L., Tse, M.S., Tan, O.K. and Hildemann, L.M. (2012). Preparation of TiO_2-Coated Polyester Fiber Filter by Spray-Coating and Its Photocatalytic Degradation of Gaseous Formaldehyde. *Aerosol Air Qual. Res.* 12: 1327–1335.

Hong, Y.C., Bang, C.U., Shin, D.H. and Uhm, H.S. (2005). Band Gap Narrowing of TiO_2 by Nitrogen Doping in Atmospheric Microwave Plasma. *Chem. Phys. Lett.* 413: 454–457.

Hong, Y.C. and Uhm, S. (2007). Production of Nanocrystalline TiO_2 Powder by a Microwave Plasma-Torch and Its Characterization. *Jpn. J. Appl. Phys.* 46: 6027–6031.

Hsieh, C.S., Zhu, H., Wei, T.Y., Chungc, Z.J., Yang, W.D. and Ling, Y.H. (2008). Applying the Experimental Statistical Method to Deal the Preparatory Conditions of Nanometric-sized TiO_2 Powders from a Two-emulsion Process. *J. Eur. Ceram. Soc.* 28: 1177–1183.

Hsieh, L.Y., Kuo, S.C., Chen, C.L. and Tsai, Y.I. (2009). Size Sistributions of Nano/Micron Dicarboxylic Acids and Inorganic Ions in Suburban PM Episode and Non-episodic Aerosol. *Atmos. Environ.* 43: 4396–4406.

Johannessen, T., Pratsinis, S.E. and Livbjerg, H. (2001). Computational Analysis of Coagulation and Coalescence in the Flame Synthesis of Titania Particles. *Powder Technol.* 118: 242–250.

Kammler, H.K., Pratsinis, S.E., Morrison, P.W. and Hemmerling, B. (2002). Flame Temperature Measurement during Electrically Assisted Aerosol Synthesis of Nanoparticle. *Combust. Flame* 128: 369–381.

Kammler, H.K., Jossen, R., Morrison, P.W., Pratsinis, S.E. and Beaucage, G. (2003). The Effect of External Electric Fields during Flame Synthesis of Titania. *Powder Technol.* 135: 310–320.

Li, M., Gonzalez-Aguilar, J. and Fulcheri, L. (2008). Synthesis of Titania Nanoparticles Using a Compact Nonequilibrium Plasma Torch. *Jpn. J. Appl. Phys*. 47: 7343–7345.

Lu, C.H., Wu, W.H. and Kale, R.B. (2008). Microemulsion-mediated Hydrothermal Synthesis of Photocatalytic TiO_2 Powders. *J. Hazard. Mater.* 154: 649–654.

McMurry, P.H. and Woo, K.S. (2002). Size Distributions of 3-100-nm Urban Atlanta Aerosols: Measurement and Observations. *J. Aerosol Med.* 15: 169–178.

Ouyang, X., Li, X., Yan, H., Mo, F. and Zhao, C. (2008a). Preparation and Characterization of Nanosized TiO_2 Powders by Gaseous Detonation Method. *Mater. Sci. Eng., B* 153: 21–24.

Ouyang, X., Li, X., Yan, H., Qu, Y. and Mo, F. (2008b). Synthesis of TiO_2 Nanoparticles from Sprayed Droplets of Titanium Tetrachloride by the Gas-Phase Detonation Method. *Combust. Explo. Shock+* 44: 597–600.

Parida, K.M. and Naik, B. (2009). Synthesis of Mesoporous $TiO_{2-x}N_x$ Spheres by Template Free Homogeneous Co-precipitation Method and their Photo-catalytic Activity under Visible Light Illumination. *J. Colloid Interface Sci.* 333: 269–276.

Pratsinis, S.E., Zhu, W.H. and Vemury, S. (1996). The Role of Gas mixing in Flame Synthesis of Titania Powders. *Powder Technol.* 86: 87–93.

Ritala, M., Leskela, M., Nykanen, E., Soininen, P. and Niinisto, L. (1993). Growth of Titanium-Dioxide Thin-Films by Atomic Layer Epitxy. *Thin Solid Films* 225: 288–295.

Seery, M.K., George, R., Floris, P. and Pillai, S.C. (2007). Silver Doped Titanium Dioxide Nanomaterials for Enhanced Visible Light Photocatalysis. *J. Photochem. Photobiol., A* 189: 25–263.

Shie, J.L., Lee, C.H., Chiou, C.S., Chang, C.T., Chang, C.C. and Chang, C.H. (2009). Photodegradation Kinetics of Formaldehyde Using Light Sources of UVA, UVC and UVLED in the Presence of Composed Silver Titanium Oxide Photocatalyst. *J. Hazard. Mater.* 155: 164–172.

Tsai, C.Y., Hsi, H.C., Kuo, T.H., Chang, Y.M. and Liou, J.H. (2013). Preparation of Cu-Doped TiO_2 Photocatalyst with Thermal Plasma Torch for Low-Concentration Mercury Removal. *Aerosol Air Qual. Res*. 13: 639–648.

Tsantilis, S., Kammler, H.K. and Pratsinis, S.E. (2002). Population Balance Modeling of Flame Synthesis of Titania Nanoparticles. *Chem. Eng. Sci.* 57: 2139–2156.

Valentin, C.D., Pacchioni, G., Selloni, A., Livraghi, S. and Giamello, E. (2005). Characterization of Paramagnetic Species in N-doped TiO_2 Powders by EPR Spectroscopy and DFT Calculations. *J. Phys. Chem. B* 109: 11414–11419.

Vijay, M., Selvarajan, V., Sreekumar, K.P., Yu, J., Liu, S. and Ananthapadmanabhan, P.V. (2009). Characterization and Visible Light Photocatalytic Properties of Nanocrystalline TiO_2 Synthesized by Reactive Plasma Processing. *Sol. Energy Mater. Sol. Cells.* 93: 1540–1549.

Wang, C.M., Wu, H. and Chung, S.L. (2006). Optimization of Experimental Conditions based on Taguchi Robust Design for the Preparation of Nano-sized TiO_2 Particles by Solution Combustion Method. *J. Porous Mater.* 13: 307–314.

Yang, Y., Mao, P., Wang, Z.P. and Zhang, J.H. (2012). Distribution of Nanoparticle Number Concentrations at a Nano-TiO_2 Plant. *Aerosol Air Qual. Res*. 12: 934–940.

Received for review, October 6, 2012
Accepted, February 4, 2013